Modality-specific tracking of attention and sensory statistics in the human electrophysiological spectral exponent

Leonhard Waschke[1,2]§, Thomas Donoghue[3], Lorenz Fiedler[4], Sydney Smith[5], Douglas D. Garrett[1,2], Bradley Voytek[3,5,6,7]#, & Jonas Obleser*[8,9]#

1 Max Planck UCL Centre for Computational Psychiatry and Ageing Research, Max Planck Institute for Human Development, 14195 Berlin, Germany
2 Center for Lifespan Psychology, Max Planck Institute for Human Development, 14195 Berlin, Germany
3 Department of Cognitive Science, University of California, San Diego, 9500 Gilman Drive, La Jolla, CA 92093, USA
4 Eriksholm Research Centre, Oticon A/S, Snekkersten, Denmark
5 Neurosciences Graduate Program, University of California, San Diego, 9500 Gilman Drive, La Jolla, CA 92093, USA
6 Halıcıoğlu Data Science Institute, University of California, San Diego, La Jolla, CA 92093, USA
7 Kavli Institute for Brain and Mind, University of California, San Diego, La Jolla, CA, USA
8 Department of Psychology, University of Lübeck, 23562 Lübeck, Germany
9 Center of Brain, Behavior, and Metabolism, University of Lübeck, 23562 Lübeck, Germany

Authors share senior authorship

§ Lead contact: Dr. Leonhard Waschke, Max Planck UCL Centre for Computational Psychiatry and Ageing Research, Max Planck Institute for Human Development,14195 Berlin, Germany, phone +49 30 82406 249, waschke@mpib-berlin.mpg.de

Conflict of interest: The authors declare no competing financial interests.

Author contributions: LW, JO, & BV designed research with contributions from LF & TD. LW, TD, & SS recorded data. LW analysed data with contributions from JO, BV, DDG, TD, & LF. LW wrote the manuscript with contributions from all authors.

Acknowledgements: LW and DDG are supported by an Emmy Noether Programme grant from the German Research Foundation (to DDG), and by the Max Planck UCL Centre for Computational Psychiatry and Ageing Research. BV is supported by the Whitehall Foundation Grant 2017-12-73, the National Science Foundation Grant BCS-1736028 and the National Institute of General Medical Sciences Grant R01GM134363-01. JO is supported by the European Research Council (ERC-CoG-2014-646696).

Abstract

A hallmark of electrophysiological brain activity is its 1/f-like spectrum – power decreases with increasing frequency. The steepness of this "roll-off" is approximated by the spectral exponent, which in invasively recorded neural populations reflects the balance of excitatory to inhibitory neural activity (E:I balance). Here, we first demonstrate that the spectral exponent of non-invasive electroencephalography (EEG) recordings is highly sensitive to general, anaesthesia-driven as well as specific, attention-driven changes in E:I balance. We then present results from an EEG experiment during which participants detected faint target stimuli in streams of simultaneously presented auditory and visual noise. EEG spectral exponents over auditory and visual sensory cortices tracked stimulus spectral exponents of the corresponding domain, while evoked responses remained unchanged. Crucially, the degree of this stimulus–brain spectral-exponent coupling was positively linked to behavioural performance. Our results highlight the relevance of neural 1/f-like activity and enable the study of neural processes previously thought to be inaccessible in non-invasive human recordings.

Introduction

Non-invasive recordings of electrical brain activity represent the aggregated post-synaptic activity of large cortical neuronal ensembles[1]. Frequency spectra of electrophysiological recordings commonly display quasi-linearly decreasing power with increasing frequency (in log/log space; see Fig 1; see refs[2,3]). In humans this decrease is super positioned by several peaks, of which the most prominent is typically in the range of alpha oscillations (~8–12 Hz; see ref[4]). The overall decrease in power as a function of frequency *f*, reflecting aperiodic as opposed to oscillatory activity and the steepness of such $1/f^{\chi}$ spectra can be captured by the spectral exponent χ, in which smaller values reflect flatter spectra.

Importantly, inter-individual differences in the steepness of human electroencephalography power spectral densities (EEG PSD), estimated by the spectral exponent χ, are related to chronological age, performance and display stable inter-individual differences[2,5–8]. Intra-individual variations in EEG spectral exponents have also been reported as a function of overall arousal level and activation[9–11]. Based on computational models and invasive recordings of neural activity, it has been demonstrated that electrophysiological spectral exponents capture the balance of excitatory and inhibitory neural activity (E:I), with lower exponents indicating increased E:I balance[12]. Although unknown at present, it is plausible that differences in non-invasive electrophysiological spectral exponents might also depict variations in E:I balance.

The sensitivity of EEG spectral exponents to broad variations in E:I can be tested utilizing the differential effects of distinct general anaesthetics on E:I. While propofol is known to result in a net increase of inhibition, ketamine results in a relative increase of excitation[13,14]. In accordance with models of single cell activity and invasive recordings[12], propofol anaesthesia should thus lead to an increase in the spectral exponent (steepening of the spectrum) and ketamine anaesthesia to a decrease (flattening).

Even if EEG spectral exponents are sensitive to unspecific variations in E:I balance, it remains unclear if specific, behaviourally relevant intra-individual E:I variations can be inferred in a similar manner. For example, animal work has highlighted a topographically confined intra-individual change in E:I balance during the selective allocation of attentional resources to one sensory domain[15–17]. This work suggests that an attentional shift towards a given sensory modality leads to desynchronized activity (i.e., reduced low-frequency oscillations and increased high-frequency power) in cortical areas that process information from the currently attended domain[18,19]. These shifts in desynchronization likely trace back to an attention-related change in E:I balance towards excitation[19,20], which is thought to manifest in a reduction of spectral exponents[12,21]. If EEG spectral exponents indeed represent a sensitive approximation of E:I balance, selective attention should also result in a topographically specific decrease of exponents.

Importantly, 1/f-like processes not only take place in the human brain, but are ubiquitous in nature[22–25]. Given that oscillatory brain activity has been shown to synchronize with oscillatory sensory inputs in a behaviourally relevant manner[26–29], this raises the question of whether a similar link might exist between the 1/f profiles of neural responses and sensory inputs. Indeed, even speech signals which are commonly linked to brain activity through correlations between oscillatory power in speech stimuli and brain activity (i.e., entrainment in the broad sense[30]) show a pronounced 1/f shape within their amplitude modulation (AM) spectrum (see e.g., ref[31]) Hence, 1/f-like sensory inputs might represent an ecologically relevant signal beyond oscillatory signals. However, it is unclear at present if the 1/f structure of sensory inputs is tracked by 1/f-like neural activity in humans. Such a link between sensory inputs and brain activity has been reported for non-human *in vitro* and *in vivo* experiments[32–34], though it is unclear at present whether this finding generalizes to humans and non-invasive recordings.

Why would the 1/f of neural activity map the 1/f characteristics of sensory input? This might trace back to the superposition of postsynaptic potentials, the main source of EEG signals[1]. Postsynaptic potentials might temporally align and scale with the magnitude of sensory stimuli and hence mimic their spectra, as has been suggested for steady state evoked potentials (e.g., ref[35]). Thus, beyond oscillatory inputs, it appears plausible that 1/f features of sensory input may also be represented in the human brain and that this representation is essential to enable behavioural performance. If the neural tracking of 1/f sensory features is non-invasively detectable in humans, this would suggest non-oscillatory neural processes underlying perception, while greatly extending the toolset of perceptual neuroscience to include a wide range of naturalistic (1/f-like) stimuli.

Here, we test the conjecture that 1/f-like EEG activity captures changes in the E:I balance of underlying neural populations. Such a non-invasive approximation of variations in human E:I would be of great value, enabling investigations of processes previously inaccessible using non-invasive imaging techniques. This includes the role of E:I in sensory processing and perception[36,37], selective attention[19] and ageing[38], and not least in disease[39–41].

We here demonstrate the sensitivity of EEG spectral exponents to variations in E:I in two ways. First, predicated on the differential effects of E:I imbalances in propofol and ketamine[13,14], we compare EEG spectra between quiet wakefulness, propofol, and ketamine anaesthesia[42] and demonstrate the potency of EEG spectral exponents to track broad intra-individual variations in E:I balance. The second builds on the critical role of E:I balance in attention. Here, we analysed data from human participants who performed a challenging multi-sensory detection task during which they had to attend to one of two concurrently stimulated sensory modalities (auditory vs. visual) in order to detect faint target stimuli. Our results demonstrate that despite constant multisensory input, selective attention entails a modality-specific reduction of spectral exponents (spectral flattening) that is in line with an increased E:I ratio. In addition to different drivers of E:I balance, we investigated the link between environmental 1/f input and 1/f-like brain activity. We tested the tracking of 1/f sensory features in 1/f EEG spectral exponents and present evidence for behaviourally relevant neural tracking of 1/f inputs.

Results

EEG spectral exponents track differential changes to E:I balance by Propofol and Ketamine

To test the sensitivity of EEG spectral exponents to physiological changes in the balance of excitatory and inhibitory neural activity (E:I balance), we contrasted spectral exponents of human EEG recordings between quiet wakefulness and anaesthesia for two different general anaesthetics: propofol and ketamine. While propofol is known to result in a net increase of inhibition, ketamine results in a relative increase of excitation[13,14]. In accordance with models of single cell activity and invasive recordings[12], propofol anaesthesia should thus lead to an increase in the spectral exponent (steepening of the spectrum) and ketamine anaesthesia to a decrease (flattening). Based on previous results, the effect of anaesthesia on EEG spectral exponents is expected to be highly consistent and display little topographical variation[10]. For simplicity, we focused on a set of 5 central electrodes that receive contributions from many cortical and subcortical sources (see Fig 1). Indeed, EEG spectral exponents increased under propofol and decreased under ketamine anaesthesia in all participants (both $p_{permuted} < .0009$, Fig 1). Thus, EEG spectral exponents are sensitive to broad changes of E:I balance in humans and increase with net inhibition.

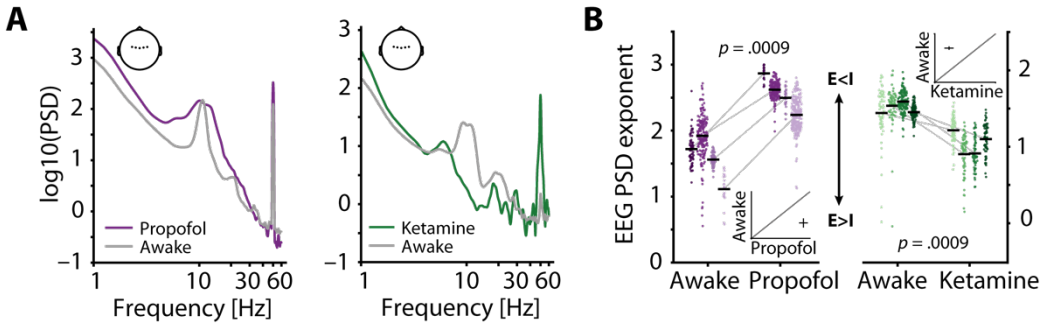

Figure 1: EEG PSD exponents track anaesthesia-induced E:I changes. (**A**) Normalized EEG spectra averaged across 4 subjects and 5 central electrodes (inset) displaying a contrast between rest and propofol (left, lilac) and ketamine anaesthesia (right, green). While propofol entails a steepened spectrum as compared to rest, ketamine is associated with spectral flattening. Note that oscillatory signals (e.g., alpha power [8–12 Hz] or line noise at 50 Hz) were estimated separately and did not contribute to spectral exponent estimates. (**B**) Pairwise scatter plots depicting subject-wise averaged EEG PSD exponents during awake rest, propofol (left) and ketamine (right). Coloured dots represent PSD exponents of 5 s snippets, black horizontal bars single subject means. Insets show 45° plots comparing awake rest and one general anaesthetic.

Behavioural performance in a multimodal detection task

Participants (N = 24) performed a challenging multisensory task during which they had to detect regular (i.e., sinusoidal) amplitude variations in streams of amplitude modulated white noise (Fig 2A). In detail, participants attended either auditory or visual noise stimuli which were always presented simultaneously and displayed amplitude modulation spectra with spectral exponents between 0 and 3 (Fig 2B). While training and adaptive adjustments of difficulty (see Methods for details) ensured that the task was challenging but doable in both modalities (average accuracy ≥ 70 %), participants performed better during visual compared to auditory trials ($t_{23} = 5.8$, $p = 7e^{-6}$, Cohen's d = 1.18; Fig 2C).

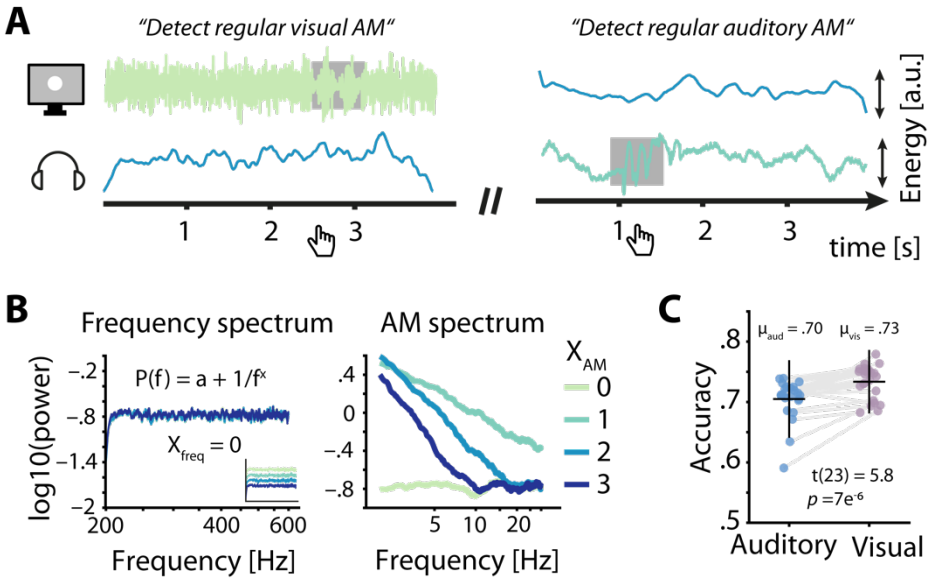

Figure 2: Task design and behavioural performance. (**A**) Participants were simultaneously presented with auditory and visual amplitude modulated (AM) noise and had to detect sinusoidal AM (grey box) in in the luminance variations of a visually presented disk (left) or in auditory presented white noise noise (right) by pressing a button. (**B**) Frequency spectra for 4 sets of AM spectra (left) demonstrate the identical flat spectra (white noise), further visualized by artificially offset spectra in the inset. AM spectra displayed spectral exponents between 0 and 3 (right). (**C**) Auditory accuracy (70 %) was significantly lower than visual accuracy (73 %).

Modality-specific attention selectively reduces the EEG spectral exponent

To further specify the sensitivity of EEG spectral exponents to specific experimental manipulations, we investigated changes in selective attention, which have been proposed to coincide with a relative increase of excitatory neural activity in sensory cortices of the attended domain. Average EEG spectral exponents for central and occipital regions of interest (see insets in Fig 3) were controlled for neural alpha power and a set of additional nuisance variables (see methods for details) and compared between auditory and visual attention using a 2 x 2 repeated measures analysis of variance. In addition to a main effect of attentional focus ($F_{1,92}$ = 12.98, p = .0005, partial eta squared = .124), this analysis revealed an interaction between attentional focus and ROI ($F_{1,92}$ = 12.91, p = .0005, partial eta squared = .123). Notably, EEG spectral exponents at occipital electrodes strongly decreased (spectra flattened) under visual compared to auditory attention (t_{23} = 7.4, p = $1e^{-7}$, Cohen's d = 1.52; see Fig 3B), while this was the case to a much lesser extent at central electrodes (t_{23} = 2.6, p = .01, Cohen's d = .54). The topographical specificity of this attention-induced spectral flattening was qualitatively confirmed by a cluster-based permutation test on the relative (z-scored) single-subject EEG spectral exponent differences between auditory and visual attention, revealing a central, negative cluster (p = .03) and an occipital positive cluster (p = .057). Thus, the selective allocation of attentional resources to one modality results in a flattening of the EEG power spectrum over electrodes typically associated with this modality, especially for occipital electrodes during visual attention.

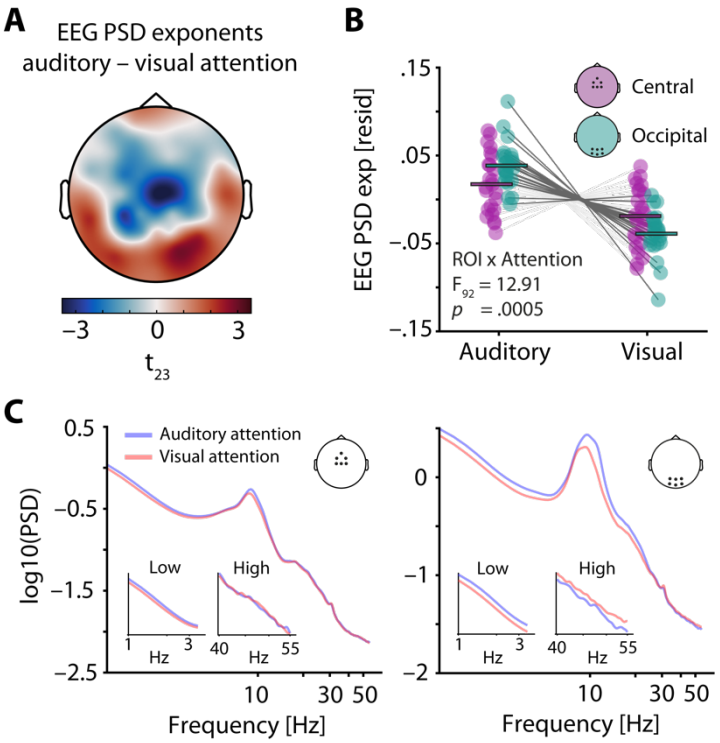

Figure 3: EEG PSD exponents track the focus of selective attention. (**A**) Average difference between EEG PSD exponents during auditory and visual attention. Note that exponents were controlled for neural alpha power and other confounding variables before subject-wise differences were calculated. A central negative and an occipital positive cluster are clearly visible. (**B**) Average central (lilac) and occipital EEG PSD exponents (teal) for auditory and visual attention (residuals shown). Horizontal bars denote the grand average. As indicated by the cross-over of connecting lines, there was a significant interaction of ROI and attentional focus. (**C**) Grand average spectra for auditory (blue) and visual attention (red), shown for a central (left) and an occipital ROI (right). Insets display enlarged versions of spectra for low and high frequencies, separately.

1/f-like stimulus properties are tracked by modality-specific changes in EEG spectral exponents

In addition to attention-related variations in brain dynamics, we probed the link between spectral exponents of sensory stimuli and EEG activity. Electrode-wise linear mixed effect models of EEG spectral exponents were used to test the relationship between the amplitude modulation (AM) spectral exponents of presented stimuli and recorded EEG activity (see model details in table S1). A main effect of auditory stimulus exponent, capturing the trial-wise positive linear relationship between auditory AM spectral exponents and EEG spectral exponents was found at a set of four central electrodes (all $z > 3.5$, all $p_{corrected} < .02$; see Fig 4A). Similarly, a positive main effect of visual stimulus exponent was present at a set of three occipital electrodes (all $z > 3.7$, all $p_{corrected} < .01$; see Fig 4A). Hence, EEG spectral exponents displayed a topographically resolved tracking of stimulus exponents of both modalities. Additionally, standardized single subject estimates of stimulus tracking at both electrode clusters identified by the mixed model approach were extracted after controlling for covariates also used in the final mixed model and revealed qualitatively similar results for both auditory ($t_{23} = 5.1$, $p = .00004$, Cohen's $d = 1.03$) and visual stimulus tracking ($t_{23} = 3.9$, $p = .0008$, Cohen's $d = .79$; see Fig 4A).

Stimulus tracking in EEG spectral exponents interacts with attentional focus

To further investigate the role of selective attention for the observed neural tracking of stimulus spectral exponents, we tested for an interaction with attentional focus within the mixed model framework. This approach revealed a positive central cluster for the interaction of auditory stimulus exponents and attentional focus, as well as an occipital cluster for the interaction of visual stimulus exponents and attentional focus (see Fig 4B). Note that t-values for the auditory stimulus x attention interaction were inverted to remove the sign change caused by the zero-centred effect coding of attentional focus. In this way, positive t-values represent evidence for an increase in stimulus tracking if attention is directed towards this modality.

As can be discerned from the topographies in Figure 4B, selective attention likely improved the tracking of stimulus spectral exponents over sensory-specific areas, separately for each sensory domain. To extract single subject estimates of the stimulus x attention interaction, we controlled for several covariates, focusing on EEG spectral exponents averaged within the

clusters that displayed significant tracking (see above). Paired t-tests comparing standardized regression coefficients that represent the strength of neural stimulus tracking revealed a significant increase of auditory stimulus tracking under auditory attention (t_{23} = 2.4, p = .03, Cohen's d = .49). Visual stimulus tracking did not significantly improve under visual attention, though the direction of the effect was the same (t_{23} = 1.0, p = .33, Cohen's d = .20). Thus, modality-specific attention was selectively associated with an improvement in the neural tracking of auditory AM stimulus spectra.

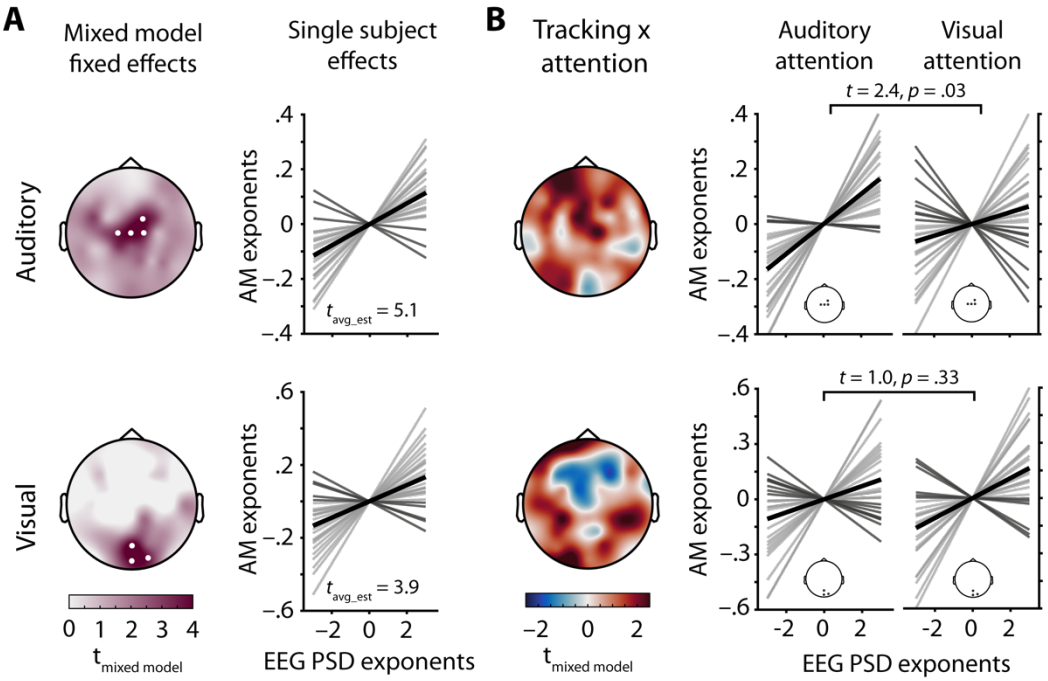

Figure 4. EEG PSD exponents track stimulus PSD exponents. (**A**) Topographies depict t-values for the main effect of stimulus PSD exponent, taken from a mixed model of EEG PSD exponents. White dots represent electrodes with significant effects after Bonferroni correction. Auditory stimulus tracking (upper row) clusters at central electrodes, visual stimulus tracking (lower row) at occipital electrodes. Line plots show single subject tracking estimates (standardized betas), dark grey lines represent negative betas, black lines the grand average. (**B**) Topographies show t-values for the interaction of attentional focus and stimulus PSD exponent, taken from the same mixed model as in A. Positive clusters appear over central (auditory) and occipital (visual) areas and represent improved tracking during selective attention to the modality in question. Line plots visualize single subject effects of selective attention on stimulus tracking for the clusters found in A (insets).

Evoked responses do not index the spectral exponent of audiovisual stimuli

To test whether conventional estimates of sensory evoked EEG activity tracked the spectral exponent of stimuli, we analysed evoked potentials (ERPs) on the single trial level. This analysis did not reveal significant ERP clusters for either auditory (p > .3) or visual (p > .2) spectral AM tracking (see Fig S2 for ERPs). The absence of such effects is visualized in supplementary Figure 2 which displays ERPs time-courses for four bins of increasing auditory as well as visual AM spectral exponents. In contrast to 1/f EEG exponents, conventional metrics of sensory evoked EEG activity were thus insensitive to the AM spectral exponents of presented stimuli.

The extent of modality-specific spectral-exponent tracking predicts behavioural performance

Next, to investigate the link between individual levels of neural stimulus tracking and behavioral performance, we computed between-subject correlations of standardized stimulus tracking betas (auditory and visual) and common metrics of behavioural performance (accuracy and

response speed, separately for both modalities) using a multivariate partial least squares analysis (PLS, see methods for details, McIntosh et al., 1996). This model revealed one significant latent variable (p = .03) that captured the low-dimensional latent space of the correlation between neural stimulus tracking and behavioural performance, which displayed a clear fronto-central topography (Fig 5A). At the overall latent level, both auditory (rho = .49, p = .016) and visual stimulus tracking (rho = .43, p = .035) were significantly correlated with performance across subjects (Fig 5B). In detail, auditory stimulus tracking was positively correlated with auditory response speed (rho = .30, CI = [.03, .64]) but negatively correlated with visual accuracy (rho = –.28, CI = [-.62, -.06]) and response speed (rho = –.36, CI = [-.73, -.17]). Analogously, visual stimulus tracking was positively linked with visual accuracy (rho = .31, CI = [.15, .68]) and response speed (rho = .35, CI = [.11, .72]; see Fig 5A), but showed no significant relationship with auditory performance. Taken together, participants who displayed stronger neural tracking of AM stimulus spectra also performed better. However, the behavioural benefit of stimulus tracking was modality-specific: performance in one sensory domain (e.g., auditory) only benefited from tracking within that domain, but not in the other (e.g., visual). Instead, visual detection performance was slower and less accurate in individuals who displayed strong neural tracking of 1/f-like auditory stimulus features.

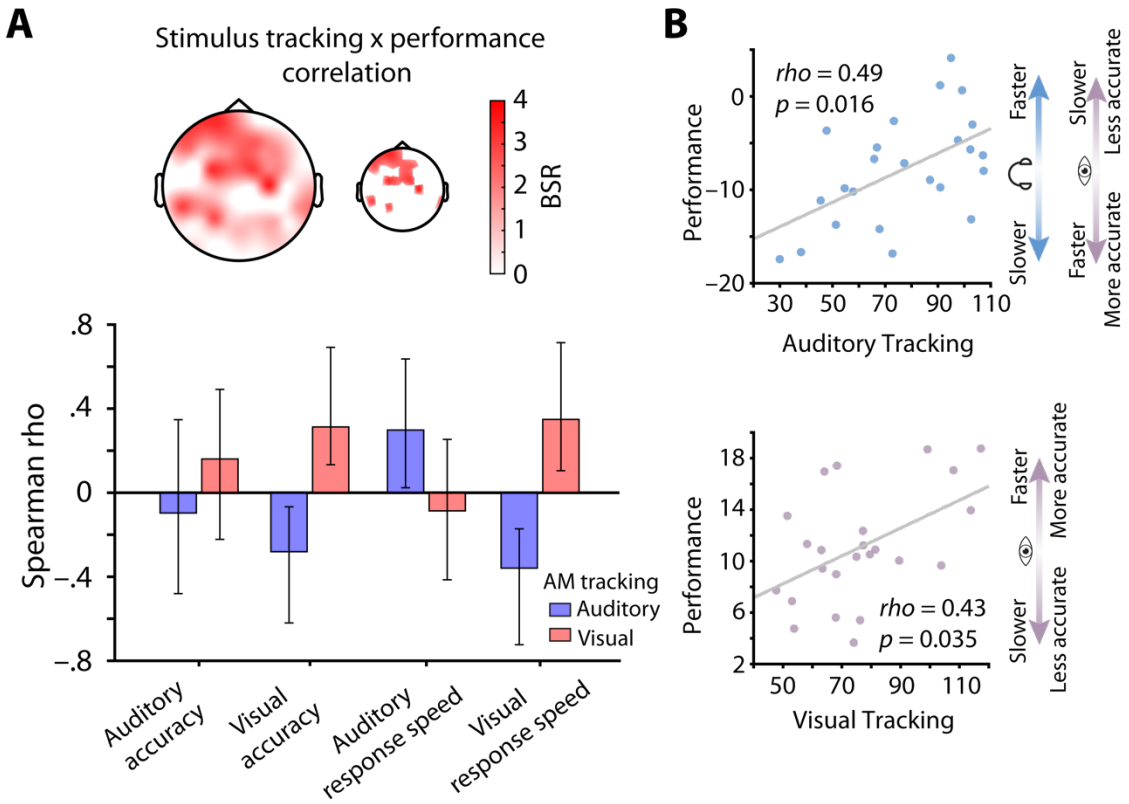

Figure 5. Stimulus tracking explains inter-individual differences in performance. (A) Results of a multivariate neuro-behavioural correlation between stimulus tracking and performance using PLS. The topography depicts bootstrap ratios (BSR) of the first latent variable and can be interpreted as z-values. Within the smaller topography, BSRs are thresholded at a BSR of 2 ($p < .05$). Bar graphs represent the correlation (Spearman rho) between auditory (blue) and visual stimulus tracking (red) with performance (accuracy as % correct and response speed; RS in s^{-1}) in both modalities. Vertical lines denote 95% bootstrapped confidence intervals. (B) Scatter plots of latent correlations between latent auditory (upper panel) and visual tracking (lower panel) with latent performance, respectively. Auditory stimulus tracking was positively linked with auditory performance but negatively linked with visual performance. Visual stimulus tracking was positively linked with visual performance. Headphones and eye symbolize auditory and visual performance, respectively.

Control analyses

To compare established metrics of early sensory processing, we contrasted evoked EEG activity of different attention conditions. Event related potentials (ERPs) after noise onset were compared between auditory and visual attention for electrodes Cz and Oz, separately. While there was no significant attention-related ERP difference found at electrode Cz, early ERP components at electrode Oz were increased during visual attention (~.08 – .15 s post-stimulus, $p_{corrected} < .05$; see supplemental Fig S3). Additionally, we subjected single trial alpha power (after partializing for EEG spectral exponents) from the ROIs shown in figure 3 to the same ANOVA (Attention (2) x ROI (2)) as EEG spectral exponents. This analysis revealed a main effect of attention ($F = 20.3$, $p = .00002$, partial eta squared = .180) as well as an interaction of attention and ROI ($F = 20.4$, $p = .00002$, partial eta squared = .181). Hence, alpha power increased from visual to auditory attention in a region-specific manner, with stronger increases over occipital cortical areas (see spectra in Fig 3C). Importantly, this attention-related change in alpha power took place over and above the observed attentional modulation of EEG spectral exponents for two reasons. First, spectral parameterization separates oscillatory and non-oscillatory components, dissecting alpha power from the spectral exponent[8]. Second, and to account for shared variance between alpha power and EEG spectral exponents that might occur due to fitting issues, we partialed each measure for the linear contributions of the other. The presence of modality-specific, attention-dependent changes despite these controls, strongly suggests that neural alpha power as well as EEG spectral exponents track distinct changes in neural activity that accompany attentional shifts, but they are not affected by the spectral content of the stimuli themselves.

Discussion

We have presented evidence for the sensitivity of the EEG spectral exponent to different neurochemical, cognitive, and sensory influences. Jointly, the results underscore the importance of 1/f brain activity for perception and behaviour. Specifically, we have shown that the EEG spectral exponent (1) reflects systemic, anaesthesia-induced changes in brain state closely linked to E:I balance, (2) captures focal attention-related changes in brain state, and (3) tracks the spectral exponent of distinct, simultaneously presented sensory stimuli. Furthermore, modality-specific stimulus tracking by EEG spectral exponents explained inter-individual variance in behavioural performance, highlighting the functional relevance of 1/f processes in human brain activity.

EEG spectral exponents as a non-invasive approximation of E:I balance

As hypothesized, propofol led to steeper spectra, while ketamine caused flattening (see Fig 1). The observed increase of spectral exponents (spectral steepening) during propofol anaesthesia is in line with previous analyses of the same dataset[9,21], as well as model-based and invasive results[12]. Spectral steepening under propofol likely traces back to strengthened inhibition via increased activity at gamma-Aminobutyric acid receptors (GABAergic activity) and hence a reduced E:I balance as compared to quiet wakefulness[13,14]. Generally in line with a previous analysis of the same data[9], ketamine-induced spectral flattening likely depicts the outcome of overall decreased inhibition that is caused by the blocking of excitatory N-methyl-D-aspartate (NMDA) receptors and an associated decrease in GABA release, resulting in an increased E:I balance[14,43].

Combined, we present strong evidence for the suitability of EEG spectral exponents as a non-invasive approximation of intra-individually changing E:I balance. While the EEG spectral exponents cannot measure E:I directly, this non-invasive approximation enables inference on neural processes previously only accessible in animals and using invasive methods. Future studies should directly compare dose-response relationships between GABA-A agonists or antagonists (e.g., Flumanezil) and the EEG spectral exponent in a larger sample.

EEG spectral exponents track modality-specific, attention-induced changes in E:I

While the EEG spectral exponent here proved indeed sensitive to systemic, exogenously driven, drug-induced alterations in E:I, we also sought to test whether it can also be leveraged to detect non-drug-induced but endogenous, attention-related variations in E:I balance. Invasive animal work suggested previously that the allocation of attentional resources should result in a topographically specific shift towards desynchronized activity and an increased E:I ratio[15,19].

Here, we observed a topographically-specific pattern of reduced EEG spectral exponents through modality-specific attention. As indexed by a significant interaction between region of interest and attentional focus, visual attention led to a flattening of EEG spectra that was especially pronounced over occipital EEG channels (cf. Fig 3). The absence of a comparable effect for auditory attention at central electrodes potentially traces back to the varying sensitivity of EEG recordings to different cortical sources. While central electrodes capture auditory cortical activity[44,45] and hence are positioned far away from their dominant source, occipital electrodes are sensitive to visual cortex activity and are directly positioned above it[46]. This topographical difference in sensitivity is further exaggerated by the scaling of volume conduction with distance, together resulting in a reduced signal to noise ratio for auditory compared to visual cortex activity[47].

Despite these important differences in the sensitivity of EEG signals, our results provide clear evidence for a modality-specific flattening of EEG spectra through the selective allocation of attentional resources. Importantly, these results cannot be explained by attention-dependent differences in neural alpha power (8–12 Hz, Fig 3), commonly interpreted as a marker of top-down guided sensory inhibition[48]. The methods we used not only separated oscillatory from 1/f-like signals, but all analyses additionally controlled for shared variance between single trial EEG alpha power and spectral exponents. Hence, attention-dependent alterations in alpha power and EEG spectral exponents occurred in parallel, but likely trace back to distinct generating sources.

The observed topographically-specific flattening of EEG spectra likely depicts subtle attention-dependent changes in E:I balance previously only accessible in invasive animal studies. Extensive work in non-human animals suggests that the allocation of attentional resources results in a thalamo-cortically induced shift of neural activity towards a desynchronized state of reduced inhibition within cortical areas that process currently attended sensory information[18,19]. Thus, EEG spectral exponents might represent a non-invasive approximation of attention-dependent intra-individual changes of E:I balance. However, future studies that combine a systemic manipulation of E:I (e.g., through GABAergic agonists) with the investigation of selective attention in humans are needed to test the links of E:I and EEG PSD exponents with greater detail. Furthermore, the separate contributions and roles of attention-related changes in neural alpha power and spectral exponents invite an exciting new line of experiments that target the neural dynamics of selective attention.

EEG spectral exponents track the 1/f features of sensory stimuli

For both modalities, the tracking of stimulus spectral exponents, based on single trials, represented a strong effect, as indicated by standardized effect size estimates (Cohen's d > .79). This set of results is especially striking given that conventional sensory-evoked responses showed no link with the spectral exponent of sensory stimuli (see Fig S2). Furthermore, potential influences of single trial performance on stimulus tracking were ruled out by a control analysis that accounted for single-trial behavioural performance and replicated the results summarized above (see Fig S4).

The neural tracking of stimulus spectra displayed distinct central and occipital topographies for auditory and visual stimuli, respectively (Fig 4). Of course, current source density transforms of sensor-level EEG topographies as used here do not represent definitive evidence for specific cortical sources. Yet, the spatial distinctiveness of both tracking patterns

strongly suggests separate cortical origins. Furthermore, the topographies of stimulus tracking strongly resemble those of sensory processing in auditory and visual sensory cortical areas, respectively[21,49]. These results are conceptually in line with findings from extracellular recordings in ferrets demonstrating the tracking of different AM spectra along the auditory pathway[50,51], and also extend previous work that analysed oscillatory human brain activity during the presentation of 1/f stimuli[52,53]. Thus, by presenting first evidence in humans, our results argue for a sensory-specific tracking of AM stimulus exponents within sensory cortical areas at the level of single trials.

Of note, auditory stimulus tracking increased significantly when participants focused their attention on auditory stimuli. In the auditory domain, this surfaced as an interaction of attentional focus and AM stimulus exponents, while a weaker if not statistically significant effect was discernible in the visual domain (Fig 4B). Hence, the selective allocation of attentional resources yielded improved tracking of 1/f-like sensory features. Due to too short, stimulus-free inter-trial intervals, we were unable to analyse if the degree of attention-induced reduction in EEG spectral exponents directly reflected the magnitude of stimulus tracking. Future research is needed to further investigate the precise link between individual averages of EEG PSD exponents, their attention-related change, and the tracking of environmental 1/f distributed inputs.

1/f stimulus tracking as a sign of non-oscillatory steady state potentials

What might constitute the mechanism that, at the level of sensory neural ensembles, gives rise to the observed link between sensory stimuli and the spectral shape of the EEG? First, it is important to emphasise that the representation of stimulus spectra in the EEG likely does not trace back to an alignment of oscillatory neural activity and oscillatory stimulus features, commonly referred to as “entrainment” in the strict sense[30]; the presented stimuli were stochastic in nature and without clear sinusoidal signals. However, neurally tracking the statistical properties of random noise time-series might emerge via a mechanism similar to the one implied in the generation of steady-state visually evoked potentials (SSVEPs[35]). The temporal sequence of transient sensory neural responses to periods of high energy in presented stimuli ultimately may result in a spectrum of neural activity whose shape is similar to the amplitude modulation spectrum of presented stimuli[35,54]. Although we do not want to rule out that sensory input of different spectral exponents directly affects E:I balance in sensory cortices, a possible underlying mechanism for such a link remains elusive at present and the data reported in the present study do not allow the direct examination of such a hypothesis. Hence, future experiments will have to determine the relationship between 1/f neural tracking and E:I balance by combining direct manipulations of E:I (e.g., GABAergic or glutamatergic drugs) with the presentation of 1/f like sensory stimuli.

Neural stimulus tracking explains inter-individual differences in performance

We used partial least squares to investigate the multivariate between-subject relationship of neural stimulus tracking to behavioural performance. Importantly, the resulting positive correlations (non-parametric) between stimulus tracking and performance cannot be explained by potential outliers in a relatively small sample (see Fig 5). Importantly, this effect was confined to each modality; while individuals who displayed high auditory tracking also displayed fast responses in auditory trials, they exhibited slower and less accurate responses on visual trials. Furthermore, participants who showed strong tracking of visual stimuli performed especially fast and accurate on visual but not auditory trials. This specificity of behavioural benefits through stimulus spectral tracking to each modality argues against the idea of attention-dependent sensory filters that entail bi-directional effects (i.e., auditory attention = visual ignoring[30,55]).

Of note, the topography of the between-subject neuro-behavioural correlations does not display peaks at the central or occipital regions that were found to show significant stimulus

tracking. However, a difference between both topographies is plausible for at least two reasons. First, the sensory stimulus tracking topographies represent fixed effects, by definition minimizing between-subject variance. In contrast, the between subject correlation of stimulus tracking and performance seeks to maximise between-subject variance, increasing the probability that a non-identical topography may be found. Second, although stimulus exponents are significantly tracked at sensor locations that point to early sensory cortices, our multisensory task required more abstract, high level representations of sensory input for accurate performance. Indeed, the fronto-central topography of the between subject correlation is suggestive of sources in frontal cortex, which have been shown to track multi-sensory information[56,57]. Furthermore, prefrontal cortex activity that gives rise to highly similar frontal topographies (Fig 5) has been found to represent information about the frequency content of auditory, visual, and somatosensory stimuli[58]. Thus, the positive link between neural stimulus tracking and performance at fronto-central electrodes points to the behavioural relevance of higher-level stimulus features represented in a supramodal fashion.

Limitations and next steps

First, attention-dependent changes in EEG spectral exponents might trace back to altered sensory-evoked responses. We argue that such a link is unlikely since differences in evoked responses were limited to the visual domain, occipital electrodes, and an early time-window (80–150 ms post noise onset, see Fig S2) that was well detached from the time-window used to extract single trial EEG spectra (starting at 500 ms post noise onset). However, this does not rule out entirely a remaining conflation of selective-attention effects and sensory-processing signatures in the EEG spectral component as no trials without sensory input were included. Although sensory input was comparable across different attention conditions (auditory & visual stimuli simultaneously), future studies are needed to further specify the link between modality-specific attention and EEG spectral exponents in the absence of sensory input.

Second, one reason for the difference in attentional improvement of stimulus tracking between modalities might lie in the difficulty of the task. Although auditory and visual difficulty were closely matched, we found significantly lower performance for auditory compared to visual trials (see Fig 2). Although we deem it unlikely that the observed difference of 3% in accuracy (70% vs. 73%) might be indicative of a meaningful difference in performance, we cannot rule out the possibility that participants needed more cognitive resources to perform the auditory task and neurally track stimulus spectra. Due to these increased demands, the effects of selective attention might have been able to amplify stimulus tracking more strongly as compared to the potentially less demanding visual condition. Future studies should investigate the role of parametric task demands for stimulus tracking, and attentional improvements thereof, by additionally recording fluctuations in pupil size during constant light conditions as a proxy measure of demand-related fluctuations in arousal[59,60].

Conclusion

The present data represent strong evidence for the feasibility of the EEG spectral exponent to represent a non-invasive approximation of intra-individual variations in states of E:I balance, be they driven globally by central-acting anaesthetics or be they driven more focally by re-allocation of selective attention. We highlight the sensitivity of EEG signals to aperiodic, 1/f-like stimulus features simultaneously in two sensory modalities and in relation to behavioural outcomes. These findings pose a transfer of results from invasive non-human animal physiology to the field of human cognitive neuroscience and set the stage for a new line of experiments that investigate intra-individual variations in brain dynamics and their role in sensory processing and behaviour using non-invasive approximations of aperiodic neural activity.

Methods

Pre-processing and analysis of EEG data under different anaesthetics

To test the effect of different central anaesthetics on 1/f EEG activity we analysed a previously published openly available dataset[42]. Sarasso and colleagues recorded the EEG of healthy individuals during quiet wakefulness and after the administration of different commonly used central anaesthetics including propofol and ketamine. Details regarding the recording protocol can be found in the original study and a recently published re-analysis[9,42]. We analysed EEG (60 channels) recordings from eight participants who either received propofol or ketamine infusion (4/4). EEG data were re-referenced to the average of all electrodes, down-sampled to 1000 Hz, and filtered using an acausal finite impulse response bandpass filter (.3–100 Hz, order 127). Next, to increase the number of samples per condition, recordings were split up into 5 second epochs. Since the duration of recordings varied between participants, this resulted in different numbers of epochs per anaesthetic and participant (propofol: 108±96 epochs; ketamine: 76±27 epochs). The power spectrum of each epoch and electrode between 1 and 100 Hz (0.25 Hz resolution) was estimated using the Welch method (*pwelch* function). The spectral parameterization algorithm (version 1.0.0; Donoghue et al., 2020) was used to parameterize neural power spectra. Settings for the algorithm were set as: peak width limits: [1 – 8]; max number of peaks: 8; minimum peak height: .05; peak threshold: 2.0; and aperiodic mode: 'fixed'. Power spectra were parameterized across the frequency range 3 to 55 Hz.

To statistically compare EEG spectral exponents between quiet wakefulness (resting state) and anaesthesia despite the low number of participants (4 per anaesthesia condition), we focused on five central electrodes (see inset in figure 1) and employed a permutation-based approach. After comparing average spectral exponents of resting state and anaesthesia recordings using two separate paired t-tests, we permuted condition labels (rest vs. anaesthesia) and repeated the statistical comparison 1000 times. Hence, the percentage of comparisons that exceed the observed t-value represents an empirically defined p-value. Note that spectra were normalized (mean centered) before visualization (Fig 1) and non-normalized power spectra can be found in the supplements (Fig S1).

EEG spectral exponents during a multisensory detection task

To investigate the dynamics of 1/f EEG activity during varying selective attention and the processing of sensory stimuli with distinct 1/f features, we recorded EEG from 25 healthy undergraduate students (21 $\pm$ 3 years old, 10 male) while they performed a challenging multisensory detection task. All participants gave written informed consent, reported normal hearing and had normal or corrected to normal vision. All experimental procedures were approved by the institutional review board of the University of California, San Diego, Human Research Protections Program. Due to below-chance level performance, one participant had to be excluded from all further analyses.

Task design and experimental procedure

The novel multisensory design used in the current study required participants to focus their attention to one modality of concurrently presented auditory and visual noise stimuli to detect brief sinusoidal amplitude variations of the presented noise (Fig 2A). Participants were asked to press the spacebar as fast and accurately as possible whenever they detected such a sinusoidal amplitude modulation (target) in the currently attended sensory domain. The experiment was divided into 12 blocks of 36 trials (432 trials total). At the beginning of each block participants were instructed to detect targets embedded in either auditory or visual noise stimuli. The to be attended modality alternated from block to block and was randomized across participants for the first block. Prior to each trial, the central white fixation cross changed its colour to green and back to white to indicate the start of the next trial. After 500 milliseconds (ms) the presentation of noise in both modalities started simultaneously. Trials lasted between 4 and 4.5 seconds, ended with the central fixation cross reappearing on the screen, and were separated by silent inter-trial intervals (uniformly sampled between 2–3.25

s). After each experimental block, participants received feedback in the form of a percentage correct score and were asked to take a break of at least one minute before continuing. Participants were seated in a quiet room in front of a computer screen. The experiment, including EEG preparation, lasted approximately 2.5 hours.

To ensure that the task was challenging but executable for all participants to a comparable degree, we combined training with an adaptive tracking procedure. In detail, participants performed 4 practice trials of each modality during which target stimuli were clearly detectable. Subsequently, participants performed 12 blocks of 36 trials each during which difficulty was adjusted by changing the modulation depth of presented targets to keep performance constantly around 70% correct.

Stimulus generation

Auditory and visual stimuli of different AM spectra were built in three steps: First, 30 second segments of white noise (sampling frequency 44.1 kHz) were generated and high-pass filtered at 200 Hz. Second, four random time-series of the same duration but differing $1/f_x$ exponent (χ = 0, 1, 2, or 3) were generated using an inverse Fourier transform and lowpass filtered at 100 Hz. Finally, separate multiplication of the white noise carrier with the modulators of different spectral exponents resulted in four signals that only varied in their AM but not in their long-term frequency spectra (see Fig 2B). The same noise was used for auditory and visual stimuli after root mean square normalization (auditory) or down-sampling to 85 Hz and scaling between 0.5 and 1 (visual). Noise stimuli presented during the experiment were cut out from the 30 s long time-series. Importantly, the AM spectra of cut out noise snippets do not necessarily overlap with the AM spectra of the longer time-series they were cut from. This difference between global and local spectra resulted in a wide distribution of AM spectra that were presented throughout the experiment. AM exponents were uncorrelated between modalities across trials. Auditory noise was presented as amplitude modulated white noise over headphones whereas visual noise was shown as luminance variations of a visually presented disk. Targets consisted of short sinusoidal amplitude modulations (6–7.5 Hz, 400 ms) and modulation depth was varied throughout the experiment to keep performance around 70 % correct. All stimuli were generated using custom Matlab® code. Auditory stimuli were presented over headphones (Sennheiser®) using a low-latency audio soundcard (Native Instruments). Visual stimuli were presented on a computer screen (85 Hz refresh rate). Both auditory and visual stimuli were presented using MATLAB® and Psychophysics toolbox (Brainard, 1997). To later analyse the relationship between EEG activity, behaviour and the AM spectra of presented stimuli, single trial stimulus spectra were extracted (1–30 Hz, .1 Hz resolution, *pwelch* in MATLAB) and parameterized to fit 1/f exponents[8]. Settings for the algorithm were set as: peak width limits: [0.5 – 12]; max number of peaks: infinite; minimum peak height: 0; peak threshold: 2.0; and aperiodic mode: 'fixed'. Power spectra were parameterized across the frequency range 1 to 25 Hz.

EEG recording and pre-processing

64-channel EEG was recorded at a sampling rate of 1000 Hz using the brainamp and the actichamp extension box (active electrodes; Brainproducts). Artifacts representing heartbeat, movement, eye blinks or saccades and channel noise were removed using independent component analysis based on functions from the fieldtrip and EEGlab toolboxes[61,62]. Components were rejected based on power spectra, time-series, topography and dipole fit. Continuous EEG signals were referenced to the average of all channels and filtered between 0.05 and 100 Hz (acausal FIR filter, order 207). Data was segmented into trials between –1 and 5 seconds relative to trial start (noise onset) and baseline corrected to the average of 1 s prior to trial start. Trials containing artifacts were removed based on visual inspection (5 $\pm$ 7 trials rejected). EEG time-series were transformed to scalp current densities using default

settings of the fieldtrip toolbox (*ft_scalpcurrentdensity*). Single trial power spectra between 1 and 100 Hz (0.5 Hz resolution) were calculated using the welch method[63]. To minimize the impact of early sensory-evoked potentials, these spectra were based on the EEG signal between 600 ms after noise stimulus onset and the appearance of a target sound. Trials during which the target appeared within 500 ms after trial start were excluded (1.5% ± 0.3% of trials). Furthermore, mirrored versions of single trial data were appended to the beginning and end of each trial before calculating spectra, effectively tripling the number of samples while not introducing new information (i.e., "mirror padding"). To approximate EEG activity in a state of awake rest despite the absence of a dedicated resting state recording, we calculated spectra based on the 500 ms before the fixation cross changed its colour, signalling the start of the next trial (same settings as above). These single trial "resting-state" spectra were averaged to reveal one resting state spectrum per participant and electrode. To estimate 1/f spectral exponents of EEG activity as well as oscillatory activity, single trial and average resting state spectra were fed into the spectral parameterization algorithm[8] and exponents were fit between 3 and 55 Hz using Python version 3.7. Trials where fits explained less than 20% of variance in EEG spectra were excluded from all further analyses (0.4% ∓ 0.6% of trials). Since we planned to control for the influence of alpha-oscillations (8–12 Hz), we extracted single-trial, single-electrode power estimates from spectral parameterization results if an oscillation was detected within the alpha frequency range. For trials where this was not the case, spectral power was averaged between 8 and 12 Hz as a substitute.

Statistical analysis

Attention tracking

To test whether the allocation of attentional resources to one sensory domain is accompanied by a selective flattening of the EEG power spectrum over related sensory areas, we followed a two-step approach. First, we used multiple linear regression to control single trial, single electrode EEG spectral exponents for a number of covariates. Specifically, and for every participant, we controlled EEG spectral exponents for the influence of auditory stimulus exponents, visual stimulus exponents, alpha power, and trial number. Next, we averaged the residuals per electrode and attention condition (auditory vs. visual attention) across trials, resulting in 2x64 EEG spectral exponent estimates per participant. The topographical pattern of the average difference between auditory and visual attention EEG spectral exponents is visualized in figure 3A. Following our hypothesis of sensory specific, attention-related flattening of EEG spectra, we averaged EEG spectral exponent residuals across a set of fronto-central (FC1, FC2, Fz, C1, C2, Cz) and parieto-occipital (P03, PO4, POz, O1, O2, Oz) electrodes to contrast activity from auditory and visual sensory areas, respectively. We modelled EEG spectral exponent as a function of ROI (central vs. occipital), attentional focus (auditory vs. visual) and their interaction, including a random intercepts and random slopes for all predictors within a linear mixed model (*fitlme* in MATLAB). Subsequently, analysis of variance (ANOVA) was used to statistically evaluate the main effect of attentional focus as well as the interaction of attentional focus and ROI.

As an additional control analysis, we tested the subject- and electrode-wise differences of EEG spectral exponents between auditory and visual attention against zero using a cluster-based permutation approach[64]. Finally, we used paired t-tests to compare attention effects between ROIs and resolve the interaction effect.

Stimulus tracking

To test the link between EEG spectral exponents and AM spectral exponents in the auditory and visual domain on the level of single trials, we used single-electrode linear mixed effect models. Model fitting was performed iteratively and hypothesis-driven, starting with an intercept only model and gradually increasing model complexity to find the best fitting

model[21,65]. After every newly added fixed effect, model fits were compared using maximum likelihood estimation. Once the final set of fixed effects was determined, a comparable procedure was used for random effects. All continuous variables were z-scored across participants (but within electrodes) before entering models, rendering the regression coefficients ® direct measures of effect size. The winning model included fixed effects for auditory stimulus exponents, visual stimulus exponents, attentional focus, trial number and resting state EEG spectral exponent (between subject factor) as well as a random intercept for all predictors and random slopes for attentional focus (see table S1). To additionally test the role of selective attention for the tracking of the presented sensory stimuli, we modelled separate interactions between auditory as well as visual stimulus exponents with attention, respectively. As models were fit for single electrodes (64 models), we corrected the resulting p-values for multiple comparisons by adjusting the family-wise error rate using the Bonferroni-Holm correction[66,67].

To arrive at single subject estimates of stimulus tracking, we chose a stepwise regression approach since including random slopes for auditory or visual stimulus exponents within the final mixed models did not improve model fit but led to convergence issues due to model complexity. Hence, on the level of single participants and electrodes, we regressed EEG spectral exponents on attentional focus, trial number, and stimulus exponents of one modality (e.g., visual). The z-scored residuals of this multiple regression were used in a second step where they were regressed on the z-scored stimulus exponent of the remaining sensory domain (e.g., auditory). The resulting beta coefficients were averaged across the electrodes that showed significant stimulus tracking within the mixed model approach, representing single subject estimates of stimulus tracking (see figure 3). By limiting data to trials from one attention condition, single subject estimates of stimulus tracking for different targets of selective attention were calculated following a similar approach.

Neuro-behavioural correlation

To investigate whether inter-individual differences in neural stimulus tracking relate to inter-individual differences in performance, we analysed correlations between single subject estimates of stimulus tracking and different metrics of behavioural performance using a multivariate partial least square approach (PLS[68,69]). In brief, so-called “behavioral PLS” begins by calculating a between-subject correlation matrix linking brain activity at each electrode with behavioural measures of interest. The size of this rank correlation matrix is determined by the number of electrodes, brain variables and behavioural variables [size = ($N_{electrodes} \times N_{brain\ variables}$) $\times N_{behavioral\ variables}$]. In the present study, we used two brain variables with 64 electrodes each (auditory and visual tracking betas) and 4 behavioural variables (auditory and visual accuracy and response speed). Next, this correlation matrix is decomposed using singular value decomposition (SVD), which results in $N_{brainvar} \times N_{behavvar}$ latent variables (8 in our case).

This approach produces two crucial outputs: (1) A singular value for every latent variable, representing the proportion of cross-block covariance accounted for by that latent variable, and; (2) a pattern of weights (n = number of electrodes) or saliencies representing the correlation strength between stimulus tracking and the used behavioural measures. The multiplication (dot product) of these weights with electrode-wise tracking estimates yields so-called “brain scores,” which here reflect the between-subject relationship of stimulus tracking and performance where positive brain scores indicate that individuals with stronger tracking display better performance. Statistical significance of brain scores and latent variables was tested through permutations of behavioural measures across individuals (5000 permutations). Additionally, the robustness of weights (saliencies) was estimated using a bootstrap procedure (5000 bootstraps, with replacement). The division of each weight by the corresponding bootstrapped standard error yields bootstrap ratios, which estimate the robustness of observed effects on an electrode-wise basis. Bootstrap ratios can be interpreted as a pseudo-Z metric. Crucially however, because multivariate PLS is run in a

single mathematical step that includes (and weights the importance of) all elements of the brain-behaviour matrix, multiple comparisons correction is neither typical nor required[68]. Furthermore, bootstraps were used to estimate 95% confidence intervals (CIs) for observed neuro-behavioural correlations.

Of note, behavioural performance metrics were calculated separately for auditory and visual attention trials. Since difficulty was adaptively adjusted throughout the experiment, leading to vastly different target modulation depths across participants, we controlled auditory and visual accuracy for the final modulation depth of the respective domain and used the residuals as a measure of performance. To furthermore exclude influences of learning and exhaustion of response speed (reaction time^{-1}) we controlled single trial response times for trial number and used averaged residuals as subject-wise indicators of response speed. Note that such an approach is especially warranted since we were specifically interested in between-subject relationships and hence the association of correlation matrices between neural tracking and performance. In accordance with such a reasoning, and to prevent outliers in our small sample to obscure results, all PLS analysis were performed using spearman correlation.

Control analyses

To test the impact of attentional focus and AM stimulus spectra on sensory evoked activity, which might potentially confound differences in EEG spectral exponents, we compared event-related potentials (ERPs) after noise onset. First, we compared noise onset ERPs between auditory and visual attention using a series of paired t-tests, separately for electrodes Cz and Oz. We corrected for multiple comparisons by adjusting p-values for the false discovery rate[70]. Next, on the level of subjects, voltage values were correlated with stimulus spectral exponents (separately for auditory and visual stimuli) across trials, per electrode, time-point and frequency (*ft_statfun_correlationT* in fieldtrip). On the second level, the resulting t-value time-series were tested against zero using a cluster-based permutation approach[64], separately for auditory and visual stimuli. Finally, to rule out task difficulty as a potential confound of stimulus tracking, we re-ran stimulus tracking mixed models including a main effect of single trial performance (correct vs. incorrect) as well as interactions between single trial performance and auditory and visual stimulus spectral exponents, respectively, to control stimulus tracking for performance and difficulty.

References

1. Buzsáki, G., Anastassiou, C. A. & Koch, C. The origin of extracellular fields and currents -- EEG, ECoG, LFP and spikes. *Nat Rev Neurosci* **13**, 407–420 (2012).
2. Voytek, B. *et al.* Age-Related Changes in 1/f Neural Electrophysiological Noise. *The Journal of Neuroscience* **35**, 13257–13265 (2015).
3. Miller, K. J., Sorensen, L. B., Ojemann, J. G. & Den Nijs, M. Power-law scaling in the brain surface electric potential. *PLoS Computational Biology* **5**, (2009).
4. Buzsáki, G., Logothetis, N. & Singer, W. Scaling Brain Size, Keeping Timing: Evolutionary Preservation of Brain Rhythms. *Neuron* **80**, 751–764 (2013).
5. Waschke, L., Wöstmann, M. & Obleser, J. States and traits of neural irregularity in the age-varying human brain. *Scientific Reports* **7**, 17381 (2017).
6. Dave, S., Brothers, T. A. & Swaab, T. Y. 1/ f neural noise and electrophysiological indices of contextual prediction in aging. *Brain Research* **1691**, 34–43 (2018).
7. Sheehan, T. C., Sreekumar, V., Inati, S. K. & Zaghloul, K. A. Signal Complexity of Human Intracranial EEG Tracks Successful Associative-Memory Formation across Individuals. *The Journal of Neuroscience* **38**, 1744–1755 (2018).
8. Donoghue, T. Parameterizing neural power spectra into periodic and aperiodic components. *Nature Neuroscience* **23**, 24 (2020).
9. Colombo, M. A. *et al.* The spectral exponent of the resting EEG indexes the presence of consciousness during unresponsiveness induced by propofol, xenon, and ketamine. *NeuroImage* **189**, 631–644 (2019).
10. Lendner, J. D. *et al.* An electrophysiological marker of arousal level in humans. *eLife* **9**, e55092 (2020).
11. Podvalny, E. *et al.* A unifying principle underlying the extracellular field potential spectral responses in the human cortex. *Journal of Neurophysiology* **114**, 505–519 (2015).
12. Gao, R., Peterson, E. J. & Voytek, B. Inferring synaptic excitation/inhibition balance from field potentials. *NeuroImage* **158**, 70–78 (2017).
13. Concas, A., Santoro, G., Serra, M., Sanna, E. & Biggio, G. Neurochemical action of the general anaesthetic propofol on the chloride ion channel coupled with GABAA receptors. *Brain Research* **542**, 225–232 (1991).
14. Franks, N. P. General anaesthesia: from molecular targets to neuronal pathways of sleep and arousal. *Nat Rev Neurosci* **9**, 370–386 (2008).
15. Kanashiro, T., Ocker, G. K., Cohen, M. R. & Doiron, B. Attentional modulation of neuronal variability in circuit models of cortex. *eLife* **6**, e23978 (2017).
16. Ni, A. M., Ruff, D. A., Alberts, J. J., Symmonds, J. & Cohen, M. R. Learning and attention reveal a general relationship between population activity and behavior. *Science* **359**, 463–465 (2018).
17. Ferguson, K. A. & Cardin, J. A. Mechanisms underlying gain modulation in the cortex. *Nat Rev Neurosci* **21**, 80–92 (2020).
18. Cohen, M. R. & Maunsell, J. H. R. Using Neuronal Populations to Study the Mechanisms Underlying Spatial and Feature Attention. *Neuron* **70**, 1192–1204 (2011).
19. Harris, K. D. & Thiele, A. Cortical state and attention. *Nature Reviews Neuroscience* **12**, 509–523 (2011).
20. Zagha, E. & McCormick, D. A. Neural control of brain state. *Current Opinion in Neurobiology* **29**, 178–186 (2014).
21. Waschke, L., Tune, S. & Obleser, J. Local cortical desynchronization and pupil-linked arousal differentially shape brain states for optimal sensory performance. *eLife* **8**, e51501 (2019).
22. Keshner, M. S. 1/f noise. *Proc. IEEE* **70**, 212–218 (1982).
23. Mandelbrot, B. B., Freeman, W. H., & Company. *The Fractal Geometry of Nature*. (Henry Holt and Company, 1983).
24. Brown, J. H. *et al.* The fractal nature of nature: power laws, ecological complexity and biodiversity. *Phil. Trans. R. Soc. Lond. B* **357**, 619–626 (2002).

25. Coensel, B. D., Botteldooren, D. & Muer, T. D. 1/f Noise in Rural and Urban Soundscapes. *ACTA ACUSTICA UNITED WITH ACUSTICA* **89**, 10 (2003).
26. Lakatos, P., Karmos, G., Mehta, A. D., Ulbert, I. & Schroeder, C. E. Entrainment of neuronal oscillations as a mechanism of attentional selection. *Science (New York, N.Y.)* **320**, 110–3 (2008).
27. Spaak, E., de Lange, F. P. & Jensen, O. Local Entrainment of Alpha Oscillations by Visual Stimuli Causes Cyclic Modulation of Perception. *Journal of Neuroscience* **34**, 3536–3544 (2014).
28. Henry, M. J., Herrmann, B. & Obleser, J. Entrained neural oscillations in multiple frequency bands comodulate behavior. *PNAS* **111**, 14935–14940 (2014).
29. Breska, A. & Deouell, L. Y. Neural mechanisms of rhythm-based temporal prediction: Delta phase-locking reflects temporal predictability but not rhythmic entrainment. *PLOS Biology* **15**, e2001665 (2017).
30. Obleser, J. & Kayser, C. Neural Entrainment and Attentional Selection in the Listening Brain. *Trends in Cognitive Sciences* **23**, 913–926 (2019).
31. Attias, H. & Schreiner, C. E. Temporal Low-Order Statistics of Natural Sounds. in *NIPS* 27–33 (MIT Press, 1997).
32. Qu, G., Fan, B., Fu, X. & Yu, Y. The Impact of Frequency Scale on the Response Sensitivity and Reliability of Cortical Neurons to 1/fβ Input Signals. *Front. Cell. Neurosci.* **13**, 311 (2019).
33. Yu, Y., Romero, R. & Lee, T. S. Preference of Sensory Neural Coding for 1 / f Signals. *Phys. Rev. Lett.* **94**, 108103 (2005).
34. Nozaki, D., Mar, D. J., Grigg, P. & Collins, J. J. Effects of Colored Noise on Stochastic Resonance in Sensory Neurons. *PHYSICAL REVIEW LETTERS* **82**, 4 (1999).
35. Norcia, A. M., Appelbaum, L. G., Ales, J. M., Cottereau, B. R. & Rossion, B. The steady-state visual evoked potential in vision research: A review. *Journal of Vision* **15**, 4 (2015).
36. Wehr, M. S. & Zador, A. M. Balanced inhibition underlies tuning and sharpens spike timing in auditory cortex. *Nature* **426**, 442–6 (2003).
37. Wörgötter, F. *et al.* State-dependent receptive-field restructuring in the visual cortex. *Nature* **396**, 165 (1998).
38. Luebke, J. I., Chang, Y.-M., Moore, T. L. & Rosene, D. L. Normal aging results in decreased synaptic excitation and increased synaptic inhibition of layer 2/3 pyramidal cells in the monkey prefrontal cortex. *Neuroscience* **125**, 277–288 (2004).
39. Dani, V. S. *et al.* Reduced cortical activity due to a shift in the balance between excitation and inhibition in a mouse model of Rett Syndrome. *Proceedings of the National Academy of Sciences* **102**, 12560–12565 (2005).
40. Cummings, D. M. *et al.* Alterations in Cortical Excitation and Inhibition in Genetic Mouse Models of Huntington's Disease. *Journal of Neuroscience* **29**, 10371–10386 (2009).
41. Lisman, J. Excitation, inhibition, local oscillations, or large-scale loops: what causes the symptoms of schizophrenia? *Current Opinion in Neurobiology* **22**, 537–544 (2012).
42. Sarasso, S. *et al.* Consciousness and complexity during unresponsiveness induced by propofol, xenon, and ketamine. *Current Biology* **25**, 3099–3105 (2015).
43. Behrens, M. M. *et al.* Ketamine-Induced Loss of Phenotype of Fast-Spiking Interneurons Is Mediated by NADPH-Oxidase. *Science* **318**, 1645–1647 (2007).
44. Huotilainen, M. *et al.* Combined mapping of human auditory EEG and MEG responses. *Electroencephalography and Clinical Neurophysiology/Evoked Potentials Section* **108**, 370–379 (1998).
45. Stropahl, M., Bauer, A.-K. R., Debener, S. & Bleichner, M. G. Source-Modeling Auditory Processes of EEG Data Using EEGLAB and Brainstorm. *Front. Neurosci.* **12**, 309 (2018).
46. Hagler, D. J. *et al.* Source estimates for MEG/EEG visual evoked responses constrained by multiple, retinotopically-mapped stimulus locations. *Hum. Brain Mapp.* **30**, 1290–1309 (2009).

47. Piastra, M. C. *et al.* A comprehensive study on electroencephalography and magnetoencephalography sensitivity to cortical and subcortical sources. *Hum Brain Mapp* hbm.25272 (2020) doi:10.1002/hbm.25272.
48. Jensen, O. & Mazaheri, A. Shaping Functional Architecture by Oscillatory Alpha Activity: Gating by Inhibition. *Frontiers in Human Neuroscience* **4**, 1–8 (2010).
49. Iemi, L. *et al.* Multiple mechanisms link prestimulus neural oscillations to sensory responses. *eLife* **8**, e43620 (2019).
50. Garcia-Lazaro, J. A., Ahmed, B. & Schnupp, J. W. H. Tuning to natural stimulus dynamics in primary auditory cortex. *Current Biology* **16**, 264–271 (2006).
51. Garcia-Lazaro, J. A., Ahmed, B. & Schnupp, J. W. H. Emergence of tuning to natural stimulus statistics along the central auditory pathway. *PLoS ONE* **6**, (2011).
52. Hermes, D., Miller, K. J., Wandell, B. A. & Winawer, J. Stimulus dependence of gamma oscillations in human visual cortex. *Cerebral Cortex* **25**, 2951–2959 (2015).
53. Teng, X., Tian, X., Doelling, K. & Poeppel, D. Theta band oscillations reflect more than entrainment: behavioral and neural evidence demonstrates an active chunking process. *European Journal of Neuroscience* **12**, 3218–3221 (2017).
54. Galambos, R., Makeig, S. & Talmachoff, P. J. A 40-Hz auditory potential recorded from the human scalp. *Proceedings of the National Academy of Sciences* **78**, 2643–2647 (1981).
55. Lakatos, P., Schroeder, C. E., Leitman, D. I. & Javitt, D. C. Predictive Suppression of Cortical Excitability and Its Deficit in Schizophrenia. *Journal of Neuroscience* **33**, 11692–11702 (2013).
56. Ghazanfar, A. & Schroeder, C. Is neocortex essentially multisensory? *Trends in Cognitive Sciences* **10**, 278–285 (2006).
57. Senkowski, D., Saint-Amour, D., Kelly, S. P. & Foxe, J. J. Multisensory processing of naturalistic objects in motion: A high-density electrical mapping and source estimation study. *NeuroImage* **36**, 877–888 (2007).
58. Spitzer, B. & Blankenburg, F. Supramodal Parametric Working Memory Processing in Humans. *Journal of Neuroscience* **32**, 3287–3295 (2012).
59. Yerkes, R. M. & Dodson, J. D. The relation of strength of stimulus to rapidity of habit-formation. *Journal of Comparative Neurology and Psychology* **18**, 459–482 (1908).
60. Zekveld, A. A., Kramer, S. E. & Festen, J. M. Pupil Response as an Indication of Effortful Listening: The Influence of Sentence Intelligibility: *Ear and Hearing* **31**, 480–490 (2010).
61. Delorme, A. & Makeig, S. EEGLAB: an open source toolbox for analysis of single-trial EEG dynamics including independent component analysis. *Journal of Neuroscience Methods* **134**, 9–21 (2004).
62. Oostenveld, R., Fries, P., Maris, E. & Schoffelen, J.-M. FieldTrip: Open source software for advanced analysis of MEG, EEG, and invasive electrophysiological data. *Computational intelligence and neuroscience* **2011**, 156869 (2011).
63. Welch, P. The use of fast Fourier transform for the estimation of power spectra: A method based on time averaging over short, modified periodograms. *IEEE Transactions on Audio and Electroacoustics* **15**, 70–73 (1967).
64. Maris, E. & Oostenveld, R. Nonparametric statistical testing of EEG- and MEG-data. *Journal of Neuroscience Methods* **164**, 177–190 (2007).
65. Tune, S., Wöstmann, M. & Obleser, J. Probing the limits of alpha power lateralisation as a neural marker of selective attention in middle-aged and older listeners. *European Journal of Neuroscience* **48**, 2537–2550 (2018).
66. Holm, S. A Simple Sequentially Rejective Multiple Test Procedure. *Scandinavian Journal of Statistics* **6**, 65–70 (1979).
67. Groppe, D., Urbach, T. & Kutas, M. Mass univariate analysis of event-related brain potentials/fields I: A critical tutorial review. *Psychophysiology* **48**, 1711–25 (2011).
68. McIntosh, A. R., Bookstein, F. L., Haxby, J. V. & Grady, C. L. Spatial Pattern Analysis of Functional Brain Images Using Partial Least Squares. *NeuroImage* **3**, 143–157 (1996).

69. Krishnan, A., Williams, L. J., McIntosh, A. R. & Abdi, H. Partial Least Squares (PLS) methods for neuroimaging: A tutorial and review. *NeuroImage* **56**, 455–475 (2011).
70. Benjamini, Y. & Hochberg, Y. Controlling the false discovery rate: a practical and powerful approach to multiple testing. *Journal of the Royal Statistical Society B* **57**, 289–300 (1995).